The Effect of the Shape of Chip Cross Section on Cutting Force and Roughness when Increasing Feed in Face Milling

János Kundrák, Károly Gyáni, Csaba Felhő, István Deszpoth
Institute of Manufacturing Science. University of Miskolc. Egyetemváros, H-3515 Miskolc, Hungary. E-mail: kundrak@uni-miskolc.hu

In this paper, the results of an investigation done with face milling are presented. The changes in cutting force and surface roughness were studied through changing the values of depth of cut and the feed per tooth. Meanwhile the permanent value of the undeformed chip cross section, which was determined (f_z and a_p), remained permanent. Increasing f_z and keeping the same value of A_c chip cross section, the ratio a_p/f_z changed in five grades from 0.5 to 8. It is shown, that if the feed is increased in the examined range so that the chip cross section is constant, then the value of the cutting force decreases, which decrease can be observed in all three force components. Accordingly,

the mechanical power required for cutting is reduced. The results of the surface roughness investigations showed that initially a significant increase can be observed in the roughness with the gradual increase of the feed (up to $a_p/f_z = 2.5$), followed by a moderate increase afterwards.

Keywords: Equation face milling, permanent chip cross section, cutting force, surface roughness

1 Introduction

Face milling is a widely-used type of high performance cutting machining. Although there are most versatile machinings regarding the position of both the cutting edges and the surfaces related to one another, due to the application ratio of high speed and complicated surfaces traditional face milling is dominant when producing parts.

Several publications on the investigation and development of face milling deal with the examination of texture, topography and cutting force. One of the newest papers on milling [1] provides a good review on the status of face milling, and especially on the features of surface texture. The method of the investigation is analysis and computer simulation. Considering geometry, the shapes of tool marks are calculated, then computer method simulates them. Schmitz et al. [2] examine the runout, always present in face mills, from the point of view of surface topography, in other words texture. However, the runout of radial direction affects not only the roughness but the dynamic relations of the process, too, because the chip cross section of each tooth is not the same. Baek et al. [3] made a mathematical model to precalculate the roughness in face milling. Hassanpour et al. [4] aimed to investigate the change in roughness, microhardness, the formation of white layer, while analysing the correlations of technological parameters and the surface integrity in hard face milling. Masmiati et al. [5] investigated the formation of residual stress and the factors influencing it, and made a mathematical model to determine the residual stress-Muñoz-Escalona and Maropoulus [6] prepared a geometrical model of the surface roughness, thus aiding estimation of the expected roughness when force milling the material Al7075-T7351. Takeuchi and Sakamoto [7] examined the tool rake and the effect of thermal expansion on the micro-geometry shape accuracy of plane surfaces. Gu et al. [8] studied the influence of spindle deformation and the equipment on the machining accuracy by FEM. Dinez and Filho [9] found that the relative position of the tool and the workpiece significantly affects tool wear and thus the milling tool-life and strongly influences surface roughness. Ng et al. [10] studied the effect of the milling direction and the tool coating in plain face milling, finding that milling downwards is more efficient. Other researchers have also examined the effect of coolant and lubricant [11], the influence of tool geometry [12] and tool wear [13].

From the literature, it can be seen that for improving the efficiency of material removal, earlier the aim was to achieve the maximum material removal rate (Q_w, mm^3/min). Now, however, there is interest in increasing the surface formation speed (A_w, mm^2/min). The increase of the surface formation speed, with permanent depth of cut can be acheived by the increase of cutting speed and feed. In the literature, there are few data for the socalled high feed processes. The increase of feed rate v_f is possible only with a proper tool geometry. Besides the standardised inserts applied for that purpose (a wiper insert or the so-called insert with parallel chamfering) there are research projects aiming to achieve a higher feed rate [14]. The essence of this is that by increasing the feed per tooth, meanwhile decreasing depth of cut a_p, the ratio a_p/f_z becomes smaller than 1 (inverse cutting). There are investigations of different positioning of the cutting edges in the milling tool and/or the application of inserts with different edge geometry consecutive in chip removal. With the higher feed, also the shape of the chip cross section changes, which affects both the surface roughness and the cutting force.

2 The typical cutting relations of face milling

The milling cutter axis is perpendicular to the machined surface and performs rotational motion with v_c (m/min) circumferential speed. The workpiece performs straight-line feed motion with v_f (m/min) feed rate. As a result of this, each point of the tool edge describes a looped epicycloid. Chip forming by the effect of v_c and v_f has different cross sections, but the difference between the minimum and maximum chip cross section (A_{cmin}, A_{cmax}) is often small. In general, the diameter of the milling cutter is a function of width of the surface to be machined as well as the position of "centrelines" relative to each other (the same centreline, big diameter, small width – nearly permanent cross section) (Fig. 1). Some important cutting parameters can be found in Tab. 1.

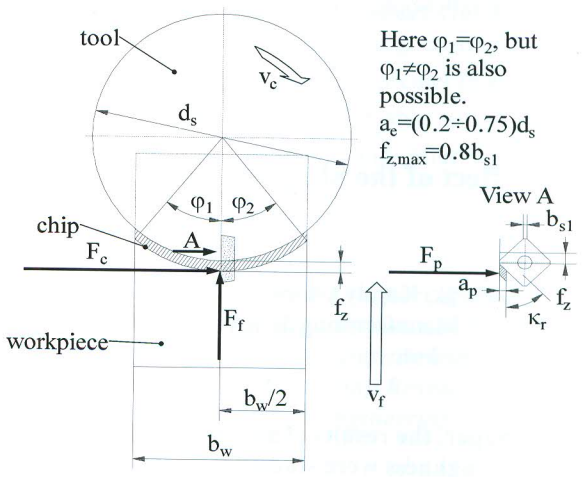

Fig. 1 The face milling cutting technology features

Tab. 1 Cutting data

Denomination	Formula	Explanation
Feed rate	$v_f=f_z\times n_s\times z_s$ (mm/min)	f_z-feed per tooth (mm) z_s-the cutter tooth number
Chip cross section (maximum)	$A_c=a_p\times f_z$ (mm^2)	
Medium chip cross section	$h_m = f_z \times b_w \times \frac{360°}{d_s \times \pi \times (\varphi_1 + \varphi_2)}$ (mm)	b_w-milling width (mm)
Material removal rate	$Q_w = \frac{b_w \times a_p \times v_f}{1000}$ (mm^3/min)	
Surface formation speed	$A_w = \frac{b_w \times v_f}{1000}$ (mm^2/min)	

The advanced milling cutter heads are equipped with inserts and use mechanical fixation. Fig. 2 shows the insert types. In the figure the conception of a_p, nose radius r_ε and cutting edge angle κ_r can be seen. Chamfer inserts with b_{s1} width are widely used, because they produce smoother surfaces than r_ε inserts with nose radius. The material of the inserts is tungsten carbide or CBN. Their clamping is mechanical, the tools with smaller diameters are fixed to the spindle directly with a taper joint, however, the milling cutters with bigger diameters are shaft-mounted versions.

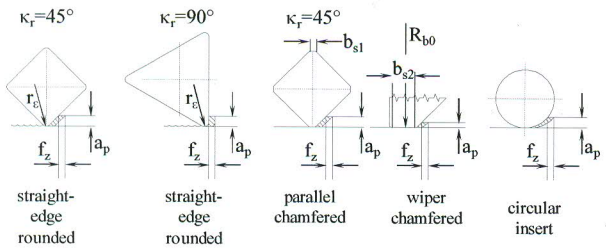

Fig. 2 Typical forms for milling cutter inserts used in the face milling and their topography

Above it was implied that one of the forecast development directions of face milling is high feed milling. To increase the feed per tooth, proper tools (tool construction + insert) are needed, since if the feed per tooth is increased with a r_ε nose radius insert, this leads to a significant increase in roughness. Among the standard inserts, the one with parallel chamfers makes it possible to increase the feed (Fig. 2). According to the literature [15], with this type of insert (Fig. 3) a maximum feed per tooth of $f_z=0.8b_{s1}$ can be achieved. To reach a higher feed per tooth special inserts have to be prepared.

3 The circumstances of milling experiments

The experiments were done with parallel chamfered inserts and smoothing grade of face milling. The aim was to examine how the surface of chip cross-section influences the roughness of the milled surface and the components of the milling force. The chip cross-section is kept constant (A_c=0.08 mm^2) and its shape is changed by a_p and f_z parameters. The characteristics of the cutting insert are demonstrated in Fig. 3.

3.1 The conditions of experimental examinations

Machine tool: Perfect Jet MCV-M8 (H) vertical machining center

Tool: SEKN1203AFTN JC5030 coated carbide insert (ISCAR). κ_r=45°; γ_o=0°; α_o=20°; b_{s1}=1.2 mm, (Fig. 3) Type of milling head: Canela 0748.90.063.

Workpiece: Normalised C45 (1.0503) carbon steel, HB 180, cut surface width: 59 mm, cut length: 50 mm.

Cutting data: cutting speed: v_c=150 m/min; spindle revolution: n_s=757.88 1/min; cut width: b_w=59 mm ($\varphi_1=\varphi_2$=69.47°); depth of cut: a_p=0.2–0.8 mm; feed per tooth: f_z=0.1-0.4 mm.

Force measurement equipment: brand of Kistler, 9257A type three-component force measurement device.

Roughness measurement equipment: AltiSurf 520 type three-dimensional surface roughness measurement device, equipped with CL2 confocal chromatic probe.

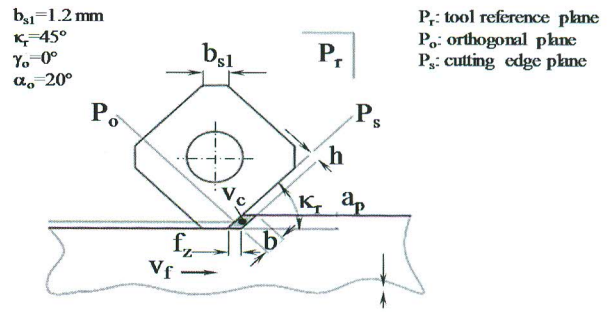

Fig. 3 The characteristics of the cutting insert applied in the experiments

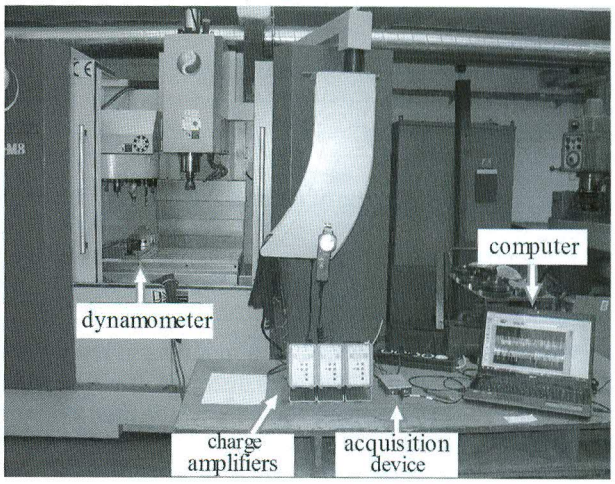

Fig. 4 Force measurement workplace

The force measurement workplace assembled from the experimental equipment is shown in Fig. 4.

3.2 Experimental method

The experiments were done with one insert (Fig. 4), with five different settings (f_z was increased while the depth of cut was chosen so that A_c remained permanent). Thus, the shape of chip cross-section was changed, which was expressed by the value of a_p/f_z ratio. The latter changed from 0.5 till 8 in five grades. Continuous force measurement was carried out during the machining, roughness was measured on each machined surface of the experimental workpieces.

4 The results of the experiment and their evaluation

4.1 The results of the measurement experiments

In the machining with rotating tools – in our experiments – the measured forces appear in the coordinate system related to the workpiece. Fig. 5 demonstrates the measured forces and their changes for one cutting period, that is in the material removal of single chip, as well as the coordinate system of force measuring system in which F_x, F_y, F_z measured force components are interpreted. On the basis of Fig. 5, the conceptual draft of the advancement of F_x, F_y, F_z forces can be drawn as a function of cutting time (Fig. 6). The theoretical shape of the F_x component can be interpreted on the basis of the points marked 1, 2 and 3 in Fig. 5a. This curve reflects the vertical (x direction) change signed F_{cx} of F_c cutting force. However, the force measured at point P at the maximum of the curve is equal to cutting force F_c (the point marked 3in Fig. 5).

The cutting period of the insert is very short because of the high cutting rate. If n_s is the number of revolution per minute of tool with diameter d_s, the time of one revolution is:

$$t_{f1} = \frac{1}{n_s} = \frac{1 \times 60}{757.88} = 0.079 \text{ s}, \quad (1)$$

From this, the cutting time is:

$$t_{cutting} = t_{f1} \frac{\varphi^\circ}{360^\circ} = 0.31 \text{ s}, \quad (2)$$

where $\varphi^\circ = \varphi_1^\circ + \varphi_2^\circ$ according to Fig. 1 $\left(\varphi_1 = \arccos \frac{b_w}{d_s} \text{ and } \varphi_2 = 180^\circ - \varphi_1 \right)$.

If t_1 is the starting time of cutting and t_2 is the finishing time:

$t_2 - t_1 = 0.031$ s

as seen in Fig.s 6 and 7.

The theoretical status of Fig. 6 modifies in reality according to Fig. 7, that is, becomes distorted. It can be seen that the curve of F_x component intersects the time axis not in the middle of the $\overline{t_1 t_2}$ distance but shifted to the right (Fig. 7).

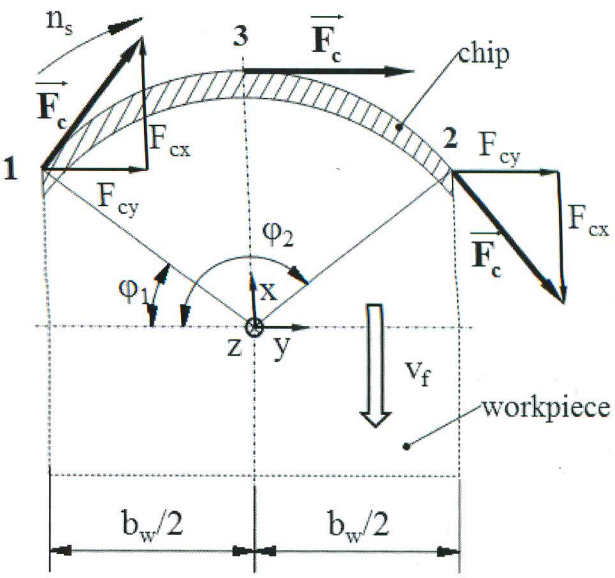

Fig. 5 The interpretation of the forces affecting the workpieces in the coordinate systém of the force measuring systém. a) changes of forces in one cutting period, b) the coordinate system of the force measuring system

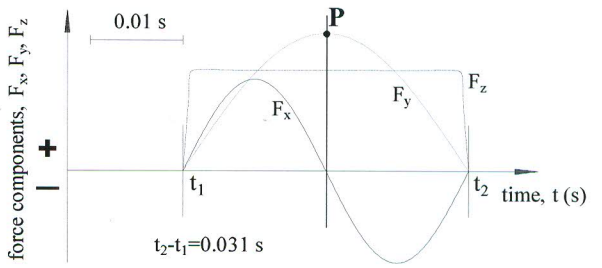

Fig. 6 The theoretically forecast advancement shape of force components on a stretched time axis

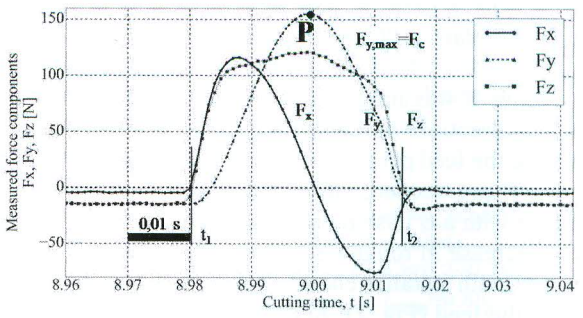

Fig. 7 One cutting period of an inserton a stretched time axis

4.2 The determination of cutting force components

The force measuring system detects and registers the force components in a coordinate system according to Fig. 5. To be precise, the analyses completed so far on feed force F_f must be accompanied by the following: the force measuring system measures not only component F_{cx} in direction x, but also F_f:

$$F_x = F_{cx} + F_f, \text{ in detail } F_x = F_c \times \sin(90^\circ - \varphi) + F_f. \quad (3)$$

On the basis of the latter, it is possible to calculate

feed force F_f.

The measurements and analysis were done for five different a_p/f_z ratios. The results are displayed in Tab. 2. There out of the resulting diagrams are displayed in Fig. 8 with their smallest, middle and highest a_p/f_z ratios. It is simpler with F_z, because it is not in xy plane of the rotation but is perpendicular to it, therefore here $F_z=F_p$.

From the results presented in Tab. 2 it can be seen that at the same cutting rate, the removal of the same chip cross section (A_c=constant) is possible with 28 % lower cutting performance, while the surface generation rate increased fourfold. (The federate increased fourfold, therefore the main machining time decreased to its fourths.)

Analysing the force measurement data, it can be stated that at a 28 % decrease of F_c, F_f decreased by 43 %, while F_p decreased by 35% in the examined range. This coincides with the general principle according to which the specific cutting force decreases with increasing chip thickness.

Presenting the measured force data (Fig. 9) it becomes clear that the shape of the chip cross section strongly affects the results of force components, while at the same time their ratio is nearly constant. For example, F_p/F_c changes between 0.77 and 0.85 in the examined range. All in all, it can be stated that the removal of the same chip volume is more advantageously performed by the higher feed per tooth.

Tab. 2 *Changes in cutting forces as a function of feed and the shape of the chip cross section (v_c=150 m/min; A_c=0.08 mm²)*

	Depth of cut	Feed per tooth	Shape of chip cross section	Ratio	Feed rate	Measured data				
No.	a_p mm	f_z mm/tooth	Planes according to Fig. 3	a_p/f_z	v_f mm/min	F_c, N	F_f, N	F_p N	P_c, kW	F_p/F_c
1	0.80	0.10	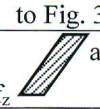	8	75.8	234.2	54.2	200.1	0.58	0.85
2	0.444	0.18	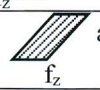	2.466	136.4	198.8	35.7	166.1	0.50	0.84
3	0.308	0.26	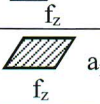	1.184	197.0	181.0	28.05	153.0	0.45	0.85
4	0.25	0.32	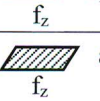	0.781	242.5	175.0	24.2	143.7	0.44	0.82
5	0.20	0.4	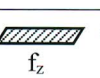	0.5	303.2	169.4	23.1	130.6	0.42	0.77

Area of the chip cross section: $A_c=a_p\times f_z$ [mm²]; feed speed: $v_f=n_s\times f_z\times z_s$ [mm/min]; cutting diameter: d_s=63 mm

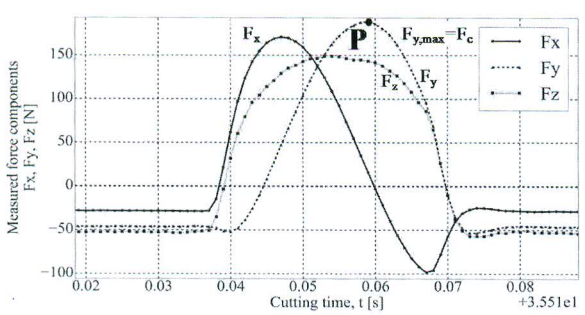

a) $a_p/f_z = 8$

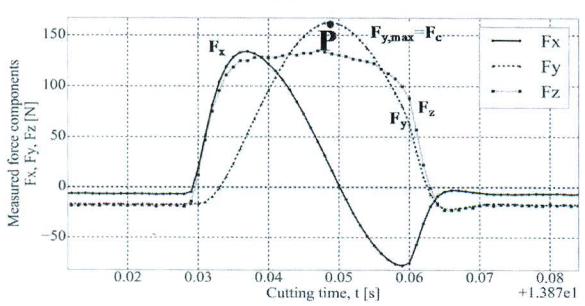

b) $a_p/f_z = 1.18$

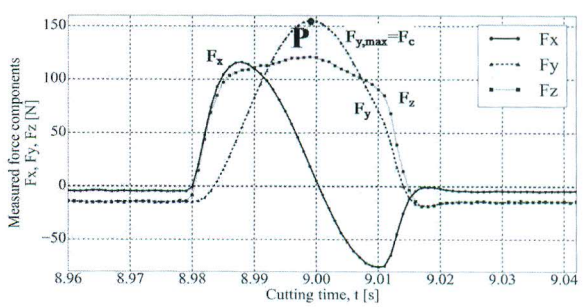

c) $a_p/f_z = 0.5$

Fig. 8 *The force components at three a_p/f_z ratios*

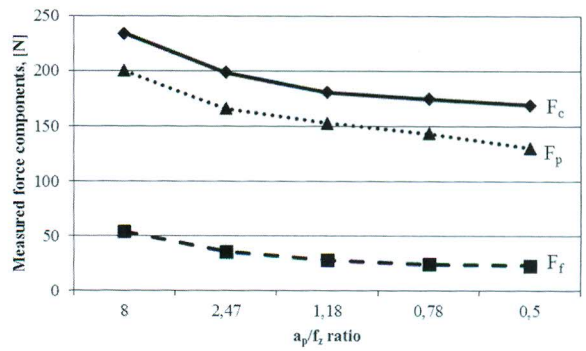

Fig. 9 *The shape of the chip cross section strongly affects the emerging forces*

At such high rates and small cutting forces (100–200 N) also dynamic and stiffness effects play a major role in the characteristic change of forces. The combination of these contributes to their characteristic advancement.

4.3 Results of roughness measurements and examinations and their evaluation

The roughness examinations were performed in 2D and 3D systems. From the 2D parameters the values of Ra, Rq and Rz are presented in this paper, along with the equivalent 3D values (Sa, Sq and S10z).

The profile diagrams and the illustrations of the topography obtained from the machined surface are displayed in Fig. 10. Out of the examined five a_p/f_z ratios three are demonstrated: the first, the middle and the last. In the 2D profiles it seems to be a characteristic tendency that increasing the feed per tooth (f_z), and the number of deep stretching grooves increases. This is disadvantageous for fatigue strain, but may be advantageous from the point of view of oil restraining capability. In 3D profiles a typical convexity can be seen by increasing roughness values, while a_p/f_z ratio is decreasing. In 3D images, too, the emergence and the increase of the deep stretching grooves mentioned above can be seen well when increasing f_z. The micro-geometrical formation of the surface can be stated to be regular.

Tab. 3 Change in roughness characteristics as function of feed and the shape of chip cross section (v_c=150 m/min; A_c=0.08 mm²)

	Depth of cut.	Feed per tooth	Shape of chip cross section	Ratio	Feed rate	Measured data						
No.	a_p mm	f_z mm/tooth	Planes according to Fig. 3	a_p/f_z	v_f mm/min	Ra µm	Sa µm	Rq µm	Sq µm	Rz µm	Sz µm	Rz/Ra
1	0.80	0.10	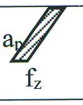	8	75.8	0.25	0.25	0.31	0.32	1.74	3.16	6.96
2	0.444	0.18	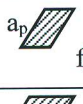	2.466	136.4	0.48	0.47	0.61	0.58	3.70	4.00	7.71
3	0.308	0.26		1.184	197.5	0.54	0.53	0.69	0.71	3.94	5.26	7.30
4	0.25	0.32		0.781	242.5	0.57	0.60	0.73	0.76	4.06	5.21	7.12
5	0.20	0.40		0.5	303.2	0.62	0.61	0.74	0.77	4.35	4.37	7.02

Cutter diameter: d_s=63 mm; feed speed: $v_f=n_s \times f_z \times z_s$ [mm/min]; milling width: b_w=59 mm

Tab. 3 contains a summary of the face milling parameters and the measurement results. It shows that the value of each index-number increases with decreasing a_p/f_z ratio. While the feed per tooth increased fourfold and a_p/f_z ratio decreased to 1/16, Ra increased 2.5-fold, Rq 2.4-fold and Rz 2.5-fold. The measurement data displayed in Tab. 3 are illustrated in Fig. 11. Rz/Ra ratio is nearly constant in the examining range.

5 Summary

Having a constant value of chip cross section and increasing the feed per tooth (with that proportionally decreasing a_p/f_z ratio), the cutting force gradually decreases, which can be observed in all three force components. With that the mechanical performance used up for chip removal decreases significantly. On this basis with further increase of feed – till the limit imposed by the tool construction and the edge geometry of cutting force – further decrease of cutting force and the needed power is expected.

In the examined face milling, increasing f_z feed per tooth, roughness gradually gets worse, to 2.5-fold a_p/f_z ratio significantly, after that with moderate intensity. In 2D profiles the pike of deep grooves directed into the material is characteristic. That is typical of the ground surfaces called "notch effect" [16]. From the point of view of fatigue, it is not advantageous. The deep grooves can be seen well in 3D topography illustration.

All in all, it can be stated that feed rate and surface rate can be increased, because power P_c decreases by increasing feed having the same chip cross section. While the feed per tooth increased fourfold and ratio a_p/f_z decreased to 1/16, the denominated 2D roughness parameters increased 2.5-fold. The increase of feed can be limited by the prescriptions in the draw of roughness values. To utilise this advantageous character of face milling, further investigations are needed in order to choose inserts with proper edge geometry for the planned feed values and to optimise insert positioning in the milling cutter.

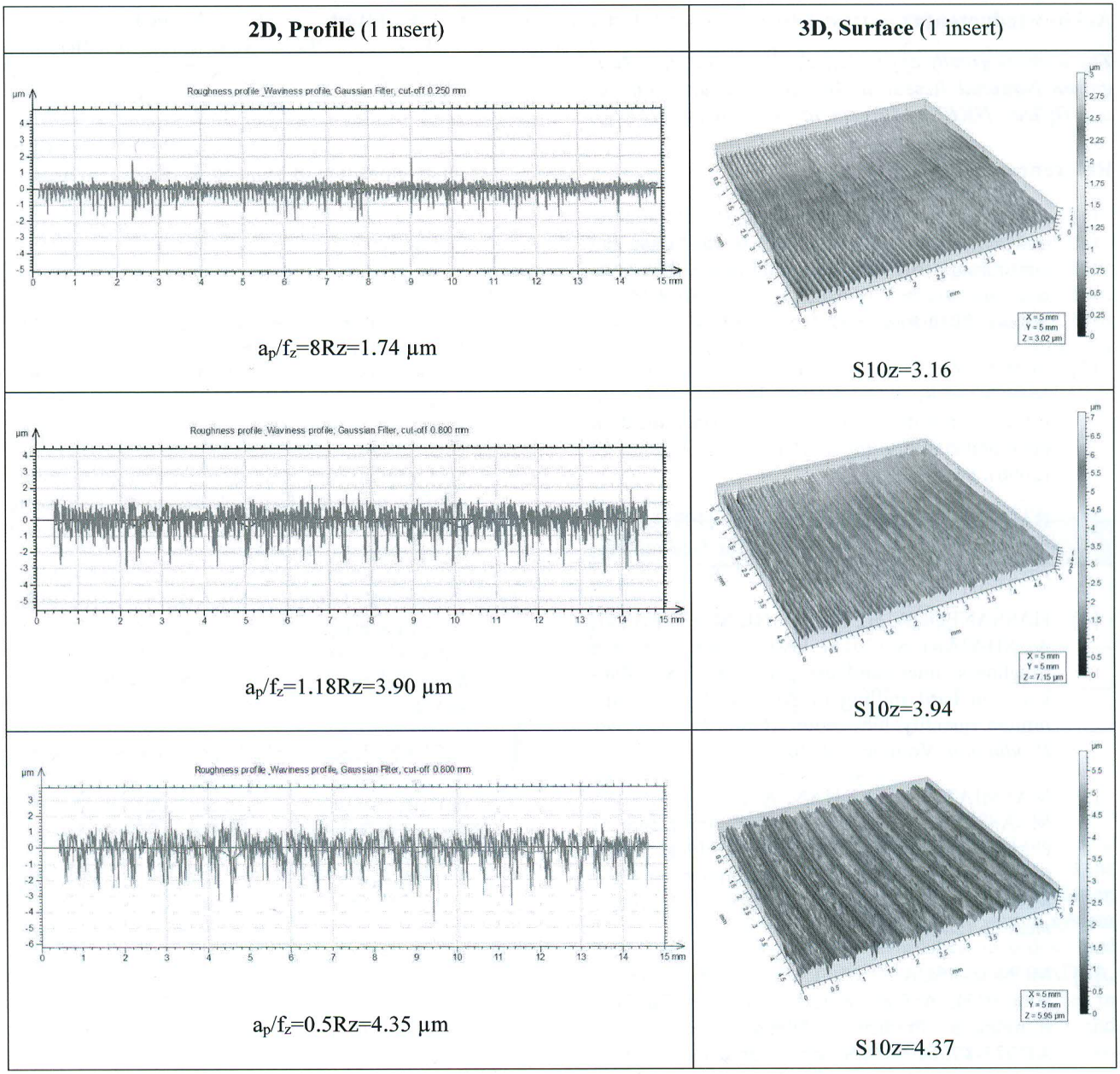

Fig. 10 *The roughness profiles and topography shots of face milling performed by 1 insert*

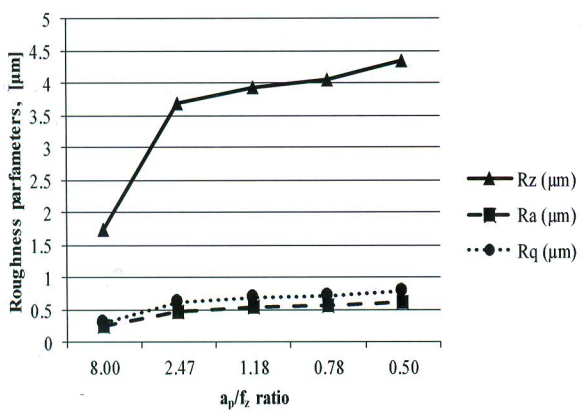

a)

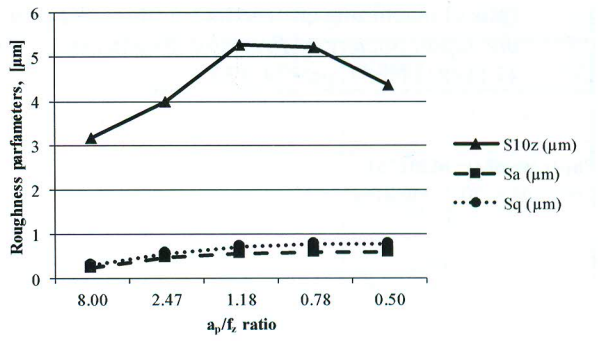

b)

Fig. 11 *The roughness results of face milling with one insert a) 2D roughness parameters, b) 3D roughness parameters*

Acknowledgments

The authors greatly appreciate the support of the Hungarian National Research, Development and Innovation Office – NKFIH (Agreement No. OTKA K 116876).

References

[1] HADAD, M., RAMEZANI, M. (2016). Modelling and analysis of a novel approach in machining and structuring of flat surfaces using face milling process, *Int. Journal of Machine Tools and Manufacture*, 2016 June, Vol. 105, pp.32-44

[2] SCHMITZ, T. L., COUEY, J., MARSH, E., MAUNTLER, N. HUGHES, D. (2006). Runout effects in milling: surface finish, surface location error and stability, *Int. J. Mach. Tools Manuf.*, 47 (2006), pp. 841–851

[3] BAEK, D. K., KO, T. J., KIM, H. S. (1997). A dynamic surface roughness model for face milling, *Precis. Eng.*, 20 (1997), pp. 171–178

[4] HASSANPOUR, H., SADEGHI, M. H., RASTI, A., SHAJARI, S. (2016). Investigation of surface roughness, microhardness and white layer thickness in hard milling of AISI 4340 using minimum quantity lubrication, *Journal of Cleaner Production*, Volume 120, 2016, pp.124–134

[5] MASMIATI, N., SARHAN, A. A.D., HASSAN, M. A. N., HAMDI, M. (2016). Optimization of Cutting Conditions for Minimum Residual Stress, Cutting Force and Surface Roughness in End Milling of S50c Medium Carbon Steel, *Measurement* 86 (2016) pp.253–265

[6] MUÑOZ-ESCALONA, P., MAROPOULOS, P. G. (2015). A Geometrical Model for Surfaces Roughness Prediction When Face Milling Al7075-T7351 With Square Insert Tools, *Journal of Manufacturing Systems*, Vol. 36, July 2015, pp.216–223

[7] TAKEUCHI, Y., SAKAMOTO, M. (1981). Analysis of machining error in face milling, *Journal of the Japan Society of Precision Engineering*, Vol. 47 (1981) No. 7, pp.874-879

[8] GU, F., MELKOTE, S. N., KAPOOR S. G., DeVOR, R. E. (1997). A Model for the Prediction of Surface Flatness in Face Milling, *J. Manuf. Sci. Eng.* Vol 119, Iss. 4A, 1997, pp.476-484

[9] DINIZ, A. E., FILHO, J. C. (1999). Influence of relative position of tool and workpiece on the tool life, tool wear and surface finish in the face milling process, *Wear*, Vol. 232, Iss. 1, September 1999, pp.67–75

[10] NG, E.-G., LEE, D. W., SHARMAN, A.R.C., DEWES, R. C., ASPINWALL, D. K., VIGNEAU, J. (2000). High Speed Ball Nose End Milling of Inconel 718, *CIRP Annals*, Vol. 49, Iss. 1, 2000, pp.41-46

[11] HRICOVA, J., NAPRSTKOVA, N. (2015). Surface roughness optimization in milling aluminium alloy by using the Taguchi's design of experiment, *Manufacturing Technology*, Volume 15, Issue 4, 1 September 2015, Pages 541-546

[12] TOMÍČEK, J., MOLOTOVNIK, A. (2016). Influence of cutting conditions on profile milling of INCONEL 738LC alloy, *Manufacturing Technology*, Volume 16, Issue 2, 1 January 2016, Pages 461-467

[13] JERSÁK, J. KAPLAN, F. (2015). Comparison of the influence of process fluids on tool life in face milling, *Manufacturing Technology*, Volume 15, Issue 6, 1 December 2015, Pages 977-984

[14] KARPUSCHEWSKI, B., BATT, S. (2007). Improvement of Dynamic Properties in Milling by Integrated Stepped Cutting, *CIRP Annals – Manufacturing Technology*, 01/2007; 56(1):85-88

[15] Sandvik Coromant: Cutting Technical Guide, C-2900:7, 2010

[16] KLOCKE, F., BRINKSMEIER, E., WEINERT, K. (2005). Capability Profile of Hard Cutting and Grinding Process, *CIRP Annals*, Vol. 54, Iss. 2, 2005, pp.22-45

Paper number: M201761